Osteoarthritis and Cartilage (2008) **16,** 480–488

doi:10.1016/j.joca.2007.08.004

Osteoarthritis and Cartilage

International Cartilage Repair Society

OARSI OSTEOARTHRITIS RESEARCH SOCIETY INTERNATIONAL

Surface ultrastructure and mechanical property of human chondrocyte revealed by atomic force microscopy

C.-H. Hsieh Ph.D.†, Y.-H. Lin Ph.D.‡, S. Lin Ph.D.§‖, J.-J. Tsai-Wu Ph.D.¶, C. H. Herbert Wu Ph.D.†* and C.-C. Jiang Ph.D., M.D.#*

† *Institute of Molecular Medicine, College of Medicine, National Taiwan University, Taipei, Taiwan*
‡ *Department of Chemistry, Tamkang University, Tamsui, Taiwan*
§ *Institute of Applied Mechanics, College of Medicine, National Taiwan University, Taipei, Taiwan*
‖ *Center for Optoelectronic Biomedicine, College of Medicine, National Taiwan University, Taipei, Taiwan*
¶ *Department of Medical Research, National Taiwan University Hospital, Taipei, Taiwan*
# *Department of Orthopedic Surgery, National Taiwan University Hospital, Taipei, Taiwan*

Summary

Objective: The mechanical properties of chondrocytes influence maintenance of the articular cartilage extracellular matrix. To differentiate the mechanical properties of chondrocytes between a young, normal modulus and an old, osteoarthritic (OA) modulus, we used an atomic force microscope (AFM) to probe the surface ultrastructure and to measure their adhesion force and stiffness.

Methods: We directly visualized a single chondrocyte cell by using AFM and quantitatively measured the dimensions of the cells.

Results: Profiles displayed heights of 1026 ± 203 and 1668 ± 352 nm for old and young cells, respectively. Contour maps revealed differences in the sizes and structures of the two groups. Mean calculated adhesion forces differed between normal and OA chondrocytes (7.06 ± 3.35 and 2.97 ± 1.82 nN, respectively), as did calculated stiffness values (0.0960 ± 0.009 and 0.0347 ± 0.005 N/m, respectively).

Conclusion: These findings suggested that the mechanical properties of normal chondrocytes substantially differed from those of OA chondrocytes. We believe this study represents the first direct characterization of the surface ultrastructure and mechanical measurements of human chondrocytes between normal and OA stages. This new approach could be a useful technique for investigating age-related changes in the properties of human chondrocytes.

Key words: Osteoarthritis, Chondrocyte, Stiffness force, Adhesion force, Atomic force microscopy.

Introduction

The articular cartilage is a unique, tough, and elastic connective tissue in joints that withstands and distributes mechanical forces. It is an avascular tissue composed of chondrocytes embedded in a highly organized extracellular matrix (ECM) of collagens, proteoglycans, and glycoproteins[1]. Chondrocytes in the cartilage detect different loading conditions, respond to mechanical signals, and thereby maintain homeostasis of the cartilaginous tissue[2–5]. They regulate the metabolic activity by means of complex biologic and biophysical interactions with the ECM that affect the development of cartilage and the progression of joint diseases and aging[6–9].

Damage to the articular cartilage causes joint dysfunction, arthritis-related disability, a limited capacity for self-repair, inflammatory arthropathy, and osteoarthritis (OA). Physiologic levels of joint loading do cause joint injury. However, impact loading of the articular cartilage, which is greater than joint loading during walking or activity but lower than damaging loading, alters the cartilaginous matrix and damages chondrocytes[10]. Experimental evidence shows that loss of proteoglycans or alteration of their organization occurs first after impact loading. The loss of proteoglycans may be due to increased degradation or decreased synthesis. Substantial loss of matrix proteoglycans decreases the stiffness of cartilage and increases its permeability. These deviations may intensify loading of the remaining macromolecular framework and collagen fibrils. Thus, the vulnerability of the tissue is increased. Moreover, these injuries may cause other matrix abnormalities other than the loss of proteoglycans, such as distortions of the collagen fibril meshwork, disruptions of collagen fibril–proteoglycan relationships, or swelling of the matrix[11]. Those conditions may hurt or kill chondrocytes as well[12,13].

Integrins, heterodimeric transmembrane glycoproteins, are adhesion-related proteins that play transmitting information from ECM to the cell through activation of cell signaling pathways[14,15]. There are at least 16 α and 9 β subunits, combining to form more than 20 specific integrin receptors. The integrin $\beta 1$ was expressed abundant in the chondrocytes and mediated the adhesion[14,16].

*Address correspondence and reprint requests to: Prof Ching-Chuan Jiang, Ph.D., M.D. or C. H. Herbert Wu, Orthopedic Surgery, National Taiwan University Hospital, 7 Chung-Shan South Road, Taipei 100, Taiwan. Tel: 886-2-2312-3456 ext. 5273; Fax: 886-2-2393-9632; E-mail: herb.wu@msa.hinet.net, ccj@ntu.edu.tw

Received 9 March 2007; revision accepted 4 August 2007.

Type II collagen is the major protein in the ECM, whereas the minor proteins are type VI, IX, X, and XI collagens[2,5,17]. Type II collagen fibers consist of many covalently cross-linked, triple-helical polypeptides that interact with the minor collagens[18]. The collagens provide the tensile strength in articular cartilage[19].

Chondrocytes can sense changes in the composition of the ECM and in response to such changes, react to maintain cartilage homeostasis[20,21]. However, the articular cartilage lacks the ability to self-heal[22]. Aging of the cartilage is characterized by its internal remodeling, as defined by constant replacement of the matrix macromolecules with new chondrocytes, which in turn causes thinning of the cartilage. Meanwhile, new chondrocytes have a decreased capability to maintain and restore articular cartilage. This lost capability, with thinning of the ECM, results in stiffness and poor biomechanical properties of the joints[47]. In the articular cartilage, aging processes that may lead to cartilaginous degeneration include fraying and softening of the articular surface, decreased size and aggregation of proteoglycan aggrecans, impaired tissue repair manifesting as decreased mitotic and synthetic activity, decreased responsiveness to anabolic growth factors, reduced synthesis of small and nonuniform aggrecans, and a reduction in functional link proteins[23].

Physical factors, such as mechanical stress, soluble mediators, and matrix composition, modulate interactions between chondrocytes and the ECM to maintain homeostasis of the articular cartilage. However, details of how these factors affect the property of chondrocytes remain unclear.

Because the atomic force microscope (AFM) permits the characterization of biologic samples ranging from a single molecule to whole cells (nanometers to micrometers), it is a powerful tool for exploring the shape of a single cell, the properties of a cellular membrane, or the interaction of intermolecular forces[24–29]. A new approach involving the AFM could be useful for investigating changes in the properties of human chondrocytes that occur with aging. The goal of this study is to use an AFM technique to differentiate the mechanical behavior of the chondrocyte between the young modulus (normal) and the old modulus (OA). The primary objective of this study was to quantitatively analyze differences in appearances and mechanical properties (e.g., stiffness, topography, and interacting forces) between a normal, young modulus and an OA, old modulus of articular chondrocytes. This new approach could be a useful technique for investigating changes in the properties of human chondrocytes with aging.

Materials and methods

CHEMICALS

Type II collagenase (Sigma, St. Louis, MO) and Dulbecco modified Eagle's medium, penicillin, and streptomycin (Life Technologies Inc., Gaithersburg, MD) were used to isolate chondrocytes. Unless specified otherwise, all chemicals are analytical grade or the best grade available. We used 10% glutaraldehyde solution (Sigma) for cell immobilization. For all experiments, ultrapure distilled water was used (18 MΩ/cm; Millipore, Bedford, MA).

ISOLATION OF HUMAN CHONDROCYTES AND CELL IMMOBILIZATION

Human articular chondrocytes were prepared from surgical specimens of patients with sports-related injury or patients with OA who needed artificial knee replacement at the ages between 21 and 81 years. Transfer of the surgical materials has been approved by the research ethics committee. The specimens were divided into two groups: normal, young (patient age, 21–45 years) and OA, old (patient age, older than 65 years).

The cartilage was cut into small pieces of 1–3 mm^3, washed with phosphate-buffered saline (PBS), and treated with 2 mg of type II collagenase per milliliter in a 37°C water bath for 4 h. The cells were washed three times with PBS and cultured in T75 flasks containing 12 ml of Dulbecco modified Eagle's medium plus 10% fetal calf serum and 1% penicillin (100 IU/ml)/streptomycin (100 μg/ml) at 37°C with 5% humidified CO_2. Human articular chondrocytes were cultured for 24 h. Before AFM measurements, the cells were covered under the glass substrate. Then, 10% of the glutaraldehyde solution was applied. The sample was incubated for 30 min at room temperature, washed with distilled water for five times (50 μl per wash), and dried in air to immobilize the cells.

ATOMIC FORCE MICROSCOPY

AFM is an important tool for studying biologic samples. With this technique, a minute tip is used as a sensor, and a cantilever serves as a transducer to measure surface and force interactions between the tip of the AFM and the sample by means of cantilever-deflection signals. This optical signal can be converted to an electric signal by using a photodiode detector with quadrants phases and then recorded on a computer. When the AFM cantilever is bent by an applied force during scanning topography or force measurement, the angle of the reflected laser beam changes and is reflected onto a photodiode detector. The position of laser spot moves on a photo-detector, inducing voltaic signal changes. These signal changes can be read out to quantitatively estimate cantilever bending. This technique allowed us to investigate differences between young and old chondrocytes using images and force measurements.

The experiments were performed by using a scanning probe microscope controlled by a probe station unit (SPA-300HV and SPI 3800N, respectively; SII Nano Technology Inc. Tokyo, Japan). Commercial silicone cantilevers (Pointprobe CONT; Nanoworld, Matterhorn, Switzerland) with a spring constant of 0.21 N/m were used to measure force strength and to obtain surface images with the contact modes of the AFM in air. The spring constant was calibrated by using the thermal resonance method in which the relationship between geometric parameters and the frequency response of the cantilever was described.

SINGLE-CELL AFM MEASUREMENT

The AFM was operated in contact mode to obtain images and measure the mechanical properties of single chondrocyte. In the scanning process, the instrument was set to apply a constant force on the cell. On each horizontal line scan, both height data and the position of the probe (deflection data) were recorded by using analysis software (SPI 3800N; Seiko Instruments Inc.) to yield complementary information. The maximum scanned image was 100 × 100 μm with a scanning speed about 20 μm/s. Acquisition time was about 50 min for one image. Then, the image was zoomed in small scale for further measurements.

Single-cell imaging experiments were repeated for three cells, and each cell was measured three times. After images were recorded, they were analyzed by offline section analysis to gain information on the topography of the sample. The valley-to-peak value R_{max} defined the difference between the maximum and minimum values of the z coordinate on the surface in the analytical area (height drop) as follows: $R_{max} = z_{max} - z_{min}$. The mean height R_{mean} defined the mean z-coordinate value on the sample surface in the analytical area as follows:

$$R_{mean} = Z_{mean} = \frac{1}{N_x N_y} \sum_{i=1}^{N_x} \sum_{j=1}^{N_y} Z_{ij}, \quad (1)$$

and $z = z_{ij} - R_{mean}$. The surface roughness value R_a was analyzed for each sample. This value defined the mean value of the surface roughness in the area being analyzed as shown in Eqs. (2) and (3):

$$R_a = \frac{1}{N_x N_y} \sum_{i=1}^{N_x} \sum_{j=1}^{N_y} |z(i,j) - z_{mean}|, \quad (2)$$

and

$$Z_{mean} = \frac{1}{N_x N_y} \sum_{i=1}^{N_x} \sum_{j=1}^{N_y} Z_{ij}. \quad (3)$$

The surface root-mean-square value R_q was calculated as the standard deviation for the z coordinate on the sample surface in the area being analyzed by using Eq. (4):

$$R_q = \sqrt{\frac{1}{N_x N_y}\sum_{i=1}^{N_x}\sum_{j=1}^{N_y}(z(i,j) - z_{mean})^2}. \quad (4)$$

ADHESION FORCE AND STIFFNESS MEASUREMENTS

The AFM was changed to the force-curve console after image scanning. In this force mode, the piezo-transducer was set to drive the cantilever to touch and retract over a predefined distance on the *z* axis as shown in Fig. 1. The *z*-axis movement of the piezo-transducer and the deflection signal from the cantilever were recorded on a force curve. When the cell-fixed substrate moved and contacted the tip of the AFM while the piezo-electric scanner was extended (point 1), a cell-contact point was established (point 2). Thereafter, an applied force deformed the cell surface.

During this approach process, the slope of the force vs the piezo-electric scanner involved the cantilever and the stiffness of the sample. Therefore, it was essential to estimate the spring constant of the cantilever to obtain the mechanical properties of cell. To estimate the stiffness of cell, the theory of equivalent force constant was applied as follows: $1/k_{total} = 1/k_{cantilever} + 1/k_{cell}$, where k_{total} is the total force constant, $k_{cantilever}$ is the spring constant of the cantilever, and k_{cell} is the stiffness of cell. On the force curve, the k_{total} could be directly measured from the slope of noncontact region as the piezo-scanner approached the tip of the AFM, and $k_{cantilever}$ could be obtained from the thermal-frequency response.

Because of the stiffness of the cell, further probe extension caused an opposing force of increasing magnitude to be generated along with increasing strain in the cell surface (points 2 and 3). Therefore, the stiffness of the cell was obtained from the part of force curve. The upward deflection of the cantilever as it bent in response to this force resulted in an increasing deflection signal. The stiffness measurement was based on the relation between the stress and strain determined under various loading modes below the stress level that caused permanent deformation[30]. The resulting slope obtained from the approach region (points 2–3) provided the local stiffness of the chondrocytes at only a few cell-surface locations. When the probe was retracted from the cell (points 3–4), the force between the probe and the sample gradually decreased until the cantilever rapidly returned to its original position. At this point, the deflection signal also returned to the original value. Adhesion occurred between the probe and the cell surface; the adhesion force caused the cantilever to bend downward, and the deflection signal fell below the original value. When the adhesion was broken (point 4), the cantilever returned to its original position (point 1), and the deflection signal of the cantilever (i.e., adhesion force) was recorded on the retraction-force curve.

All force measurements were obtained at a position on the cell surface in the $10 \times 10\text{-}\mu m^2$ area. The time necessary to acquire one set of approach and retraction-force curves was 5 s.

FLOW CYTOMETRY ASSAY

Surface marker expression on chondrocytes was quantified by flow cytometric analysis according to a previously described protocol[31]. In summary, chondrocytes were isolated from surgical specimens of patients with normal or OA groups as described above. The chondrocytes were expanded *in vitro* for three passages to ensure viability and consistency of each batch of the cells. Cells (10^6/sample) were washed three times in cold PBS and collected by brief centrifugation. After centrifugation, the cells were blocked by incubating with 2% fetal bovine serum (FBS)/PBS for 20 min. After three washes by PBS and centrifugation, the cells were incubated with 5 μl of the fluorescein isothiocynate (FITC)-conjugated anti-type II collagen mAb (CHEMICON International Inc.) and the phycoerythrin (PE)-conjugated anti-beta I integrin mAb (Clone 4B4, Beckman Coulter) for 20 min in the dark at 4°C. Control samples were incubated with mouse IgG1-FITC or IgG2-PE alone. Dead cells and debris were excluded by gating live chondrocytes on forward and 90° light scatter. Because alteration of cell membrane permeability occurs in viable cells before apoptosis takes place, we did not use propidium iodide (PI) to gate out dead cells. The double stained cells were performed in a fluorescence-activated cell sorter and analyzed using a Cell-Quest flow cytometer (Becton Dickinson, Franklin Lakes, NJ, USA).

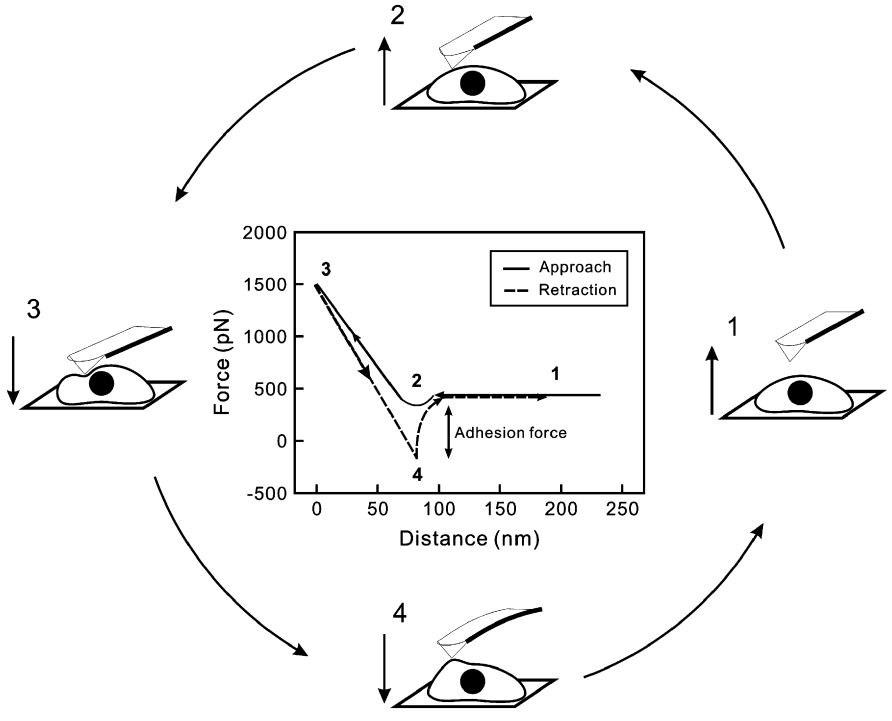

Fig. 1. Schematic shows a typical cycle for force measurement. Arrowheads indicate the relative position of the surface of the chondrocyte with respect to the tip of the AFM. For the approach (solid line), as the piezo-scanner is moved toward the tip of the AFM at constant velocity from point 1 to point 2, the attractive force pulls down the cantilever, which jumps to contact the surface at point 2. As the cantilever approaches the sample, it bends upward until it reaches point 3. For retraction (dotted line), when the tip reaches point 3, the piezo-scanner is moved away from the tip, and the cantilever begins to retract. As it does so, it bends downward until it reaches point 4. The tip–sample complex starts to break from point 4. A sharp, adhesive pull-off of approximately 150 pN, a specific tip–sample interaction, is observed in the retract trace. Finally, the cantilever returned to its original equilibrium state at point 1.

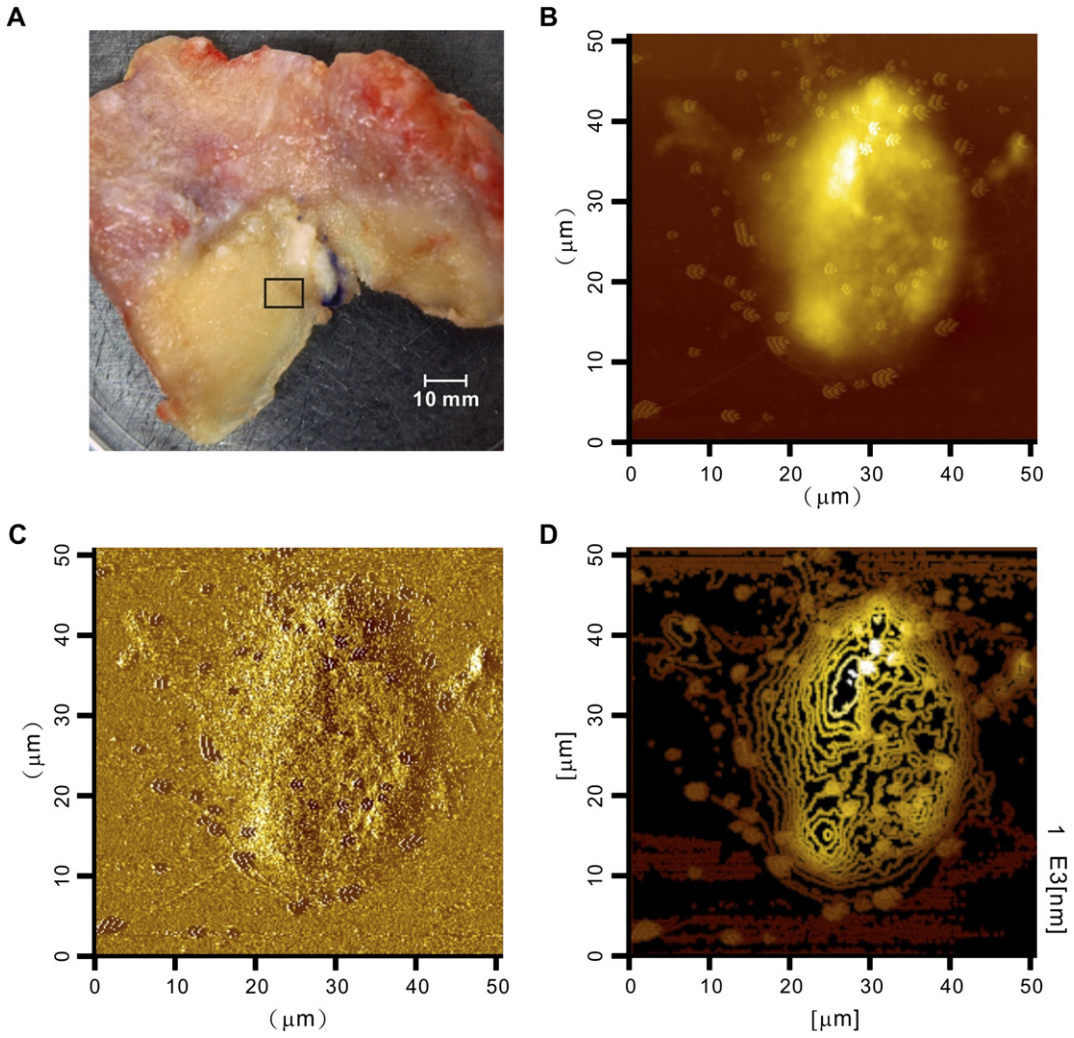

Fig. 2. Observations with AFM. A chondrocyte is isolated from OA cartilage. Square indicates the isolation area (A). A single chondrocyte is displayed on the height image (B), phase image (C), and contour map (D). Scale bar = 10 mm.

Results

AFM IMAGING OF CHONDROCYTES

Figure 2(A) shows cartilage from a patient with OA. Chondrocytes were isolated from the square area. The single chondrocyte was observed directly under the AFM and presented on a height image [Fig. 2(B)], phase image [Fig. 2(C)], and contour map [Fig. 2(D)]. Figure 2 shows differences observed between normal and OA chondrocytes after cell immobilization under the AFM in the contact mode.

A single-cell AFM image (scanning area $50 \times 50\ \mu m^2$) provided topographic information about OA [Fig. 3(A)] and normal [Fig. 3(B)] cells. Coverage areas of the OA and normal cells were 630.5 ± 28.1 and $505.6 \pm 25.6\ \mu m^2$, respectively. The maximum-height image allowed for accurate measurements of single-cell dimensions from the corresponding cursor profiles A and B, as indicated in Fig. 2. Measured heights of the old and young cells were 1026 ± 203 nm and 1668 ± 352 nm, respectively. The contour map indicated the ultrastructure of the chondrocyte and revealed differences in the sizes and structures between the old and young groups. Zooming the scale to $10 \times 10\ \mu m^2$ for every cell permitted further analysis. Table I shows parameters of the surface structure of the old and young groups.

FORCE-CURVE ANALYSIS OF CHONDROCYTES

Figure 4 shows representative examples of the force–distance curves acquired with the systems used to investigate the surface properties of the groups and the load–displacement curves recorded with different cantilever deflections. No noticeable pull-off event was observed with the tip-glass system [Fig. 4(A)]. This control experiment was used to calibrate the tip with the same cantilever on a glass surface, which acted as a rigid body to compare the low-stiffness cell sample. With the tip-OA [Fig. 4(B)] and tip-normal [Fig. 4(C)] chondrocyte systems, clear force curves were present and demonstrated relative stiffness of the cell surface (approach region) and an adhesion force between the tip of the AFM and the cell surface (retraction region).

When we analyzed the retraction trace of the force curves, we were able to determine the number of adhesion events and the forces required to break each adhesion. The load distances were measured from 300 to −50 and −80 nm for

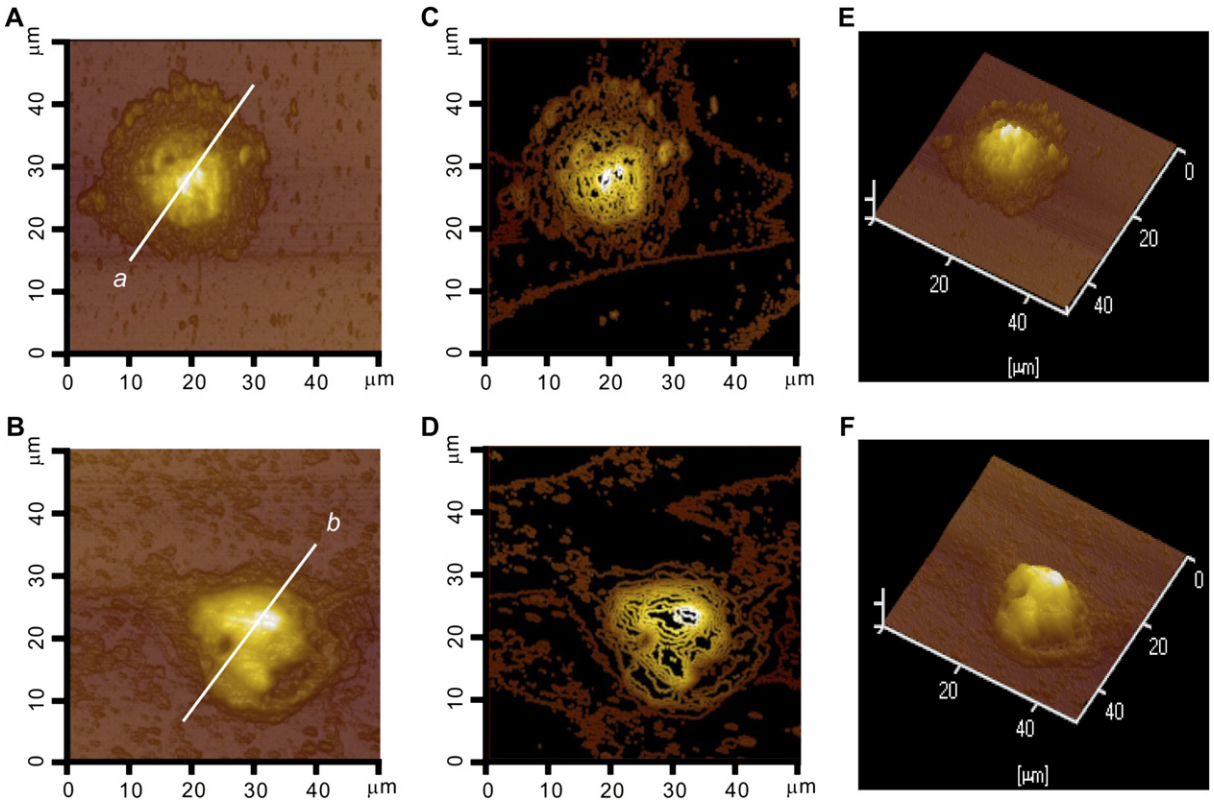

Fig. 3. Topographic AFM images of single old (A, C, and E) and young (B, D, and E) chondrocytes. Images were acquired by zooming to the maximum 100 × 100-μm scanned area (A and B, two-dimensional) and contour maps (C and D). Bar = 10 μm.

the old and young groups, respectively. Mean adhesion forces and stiffness forces calculated from the 80 and 250 sets of data are shown in Table II.

MECHANICAL PROPERTIES OF CHONDROCYTES

Figure 5 shows histograms and corresponding Gaussian distribution curves for adhesion force in the old and young groups. Each measurement was based on a 10 × 10-μm scanned area, and each adhesion that ruptured as a result of retraction of the tip from the cell surface was characterized by using the force curve. The two distribution curves on the histograms were wider for the normal chondrocytes than for the OA chondrocytes, and the peak of the old group was slightly higher than that of the young group.

Figure 6 shows histograms and corresponding Gaussian distribution curves for the stiffness of old and young chondrocytes. Peaks of the distribution curves for the old and young groups were 0.045 and 0.102, respectively. The peak widths were nearly the same.

Table I
Statistical analysis of cellular surface topographies of old and young chondrocytes

	Old chondrocytes	Young chondrocytes
Scanning area (μm^2)	630.5 ± 28.1	505.6 ± 25.6
Maximum height	1026 ± 203	1668 ± 352
Surface roughness (R_a)	788.6 ± 223.2	279.5 ± 49.7
Valley to peak (R_{max})	105.5 ± 46.0	1401.7 ± 210.4
Root mean square (R_q)	135.6 ± 58.0	343.0 ± 50.3
Mean height (R_{mean})	246.3 ± 40.2	631.7 ± 171.7

THE CELL-ASSOCIATED MATRIX OF CHONDROCYTES

Flow cytometric analysis of cell-associated matrix: integrin β1 and type II collagen in the OA chondrocytes (65, 68, 76, 79 and 81 year-old-patients) and in the normal chondrocytes (21, 24, 26, 31 and 35 year-old-patients). The chondrocytes were expanded *in vitro* for three passages to ensure viability and consistency of each batch of the cells. As shown in Fig. 7, surface expressions of integrin β1 and type II collagen were higher in the normal chondrocytes than that in the OA chondrocytes.

Discussion

Chondrocytes can produce and maintain the ECM of cartilage. They secrete the triple helix form of type II collagen. The globular ends are cleaved off, and the resulting linear, insoluble molecules are assembled into collagen fibers. Topographic AFM flash images of single chondrocyte show that the triple-helical components are distributed around the chondrocyte. The components were not clear in this work, but the components seem like the collagens secreted by chondrocyte.

The ability to image and then study the surface of living cells is one of the important advantages of using the AFM for biologic investigation. Our results revealed three obvious differences.

First, the mean maximum height differed between OA (1026 ± 203 nm) and normal chondrocytes (1668 ± 352 nm). This finding also represented low and high expressions of surface protein to interact with the ECM.

Second, differences were smaller between the highest and the lowest heights of OA chondrocytes compared

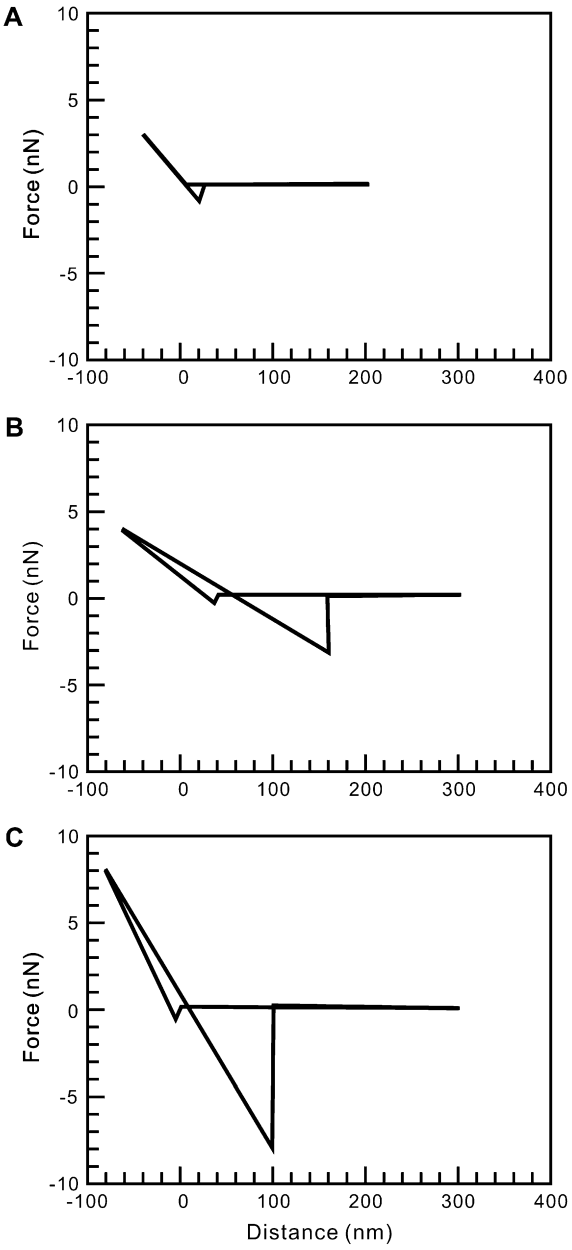

Fig. 4. Force–distance curves acquired with three systems. With the tip-glass (A), no clear pull-off event was observed. The tip-OA (B) and tip-normal (C) chondrocyte systems demonstrated the relative stiffness of the cell surface (approach curve), with a noticeable adhesion force between the tip of the AFM and the cell surface (retraction curve).

with normal chondrocytes. The peak-to-valley values were 1401.7 ± 210.4 and 105.5 ± 46.0 nm in normal and OA chondrocytes, respectively.

Third, the three-dimensional morphologies emphasized the main features of chondrocyte cells. The roominess of OA chondrocytes smoothed their roll, and they had a round nucleus surrounded by cytoplasm [Fig. 3(A), (C), and (E)]. Contrary to the OA chondrocytes, normal chondrocytes had a violent roll, which indicated a rigid cell structure in the corresponding cursor profile [Fig. 3(B), (D), and (F)]. Comparing the topography on AFM images, we found that

Table II
Comparison of adhesion forces and stiffness measurements of old and young chondrocytes

Sample	Adhesion force (nN)	Stiffness (N/m)
OA	2.972 ± 1.82	0.0347 ± 0.005
Normal	7.061 ± 3.35	0.0960 ± 0.009

the structural parameters of the small, young modulus (cell coverage area, $505.6 \pm 25.6\ \mu m^2$) were integrated with the macromolecules under the cellular membrane and that the old modulus (cell coverage area, $630.5 \pm 28.1\ \mu m^2$) was relatively incohesive. Surface proteins, including proteoglycan, lip-protein, and glycoprotein, could serve as receptors and co-receptors of important cytokines, growth factors, and ECM components. The apparent difference in roughness between OA (mean roughness, 246.3 ± 40.2 nm) and normal (mean roughness, 631.7 ± 171.7 nm) chondrocytes was strong evidence of cartilaginous degeneration resulting from decreased amounts of surface protein or macromolecules. In addition, small trihelical structures were observed around the edge of the cell [Fig. 2(B) and (C)]; this could be an evidence of matrix released from the OA chondrocytes to form ECM.

Aging is reported to cause changes in the mechanical properties of articular cartilage[32]; in the molecular composition, structure, and organization of the cartilaginous matrix[33–35]; in the synthetic and metabolic activity of chondrocytes[36,37]; and in their responsiveness to growth factor[38,39].

AFM has been used not only to image nanometer-scaled biologic samples but also to measure their mechanical properties by using the force-curve mode of the instrument. The attachment of cells to other cells or to an ECM plays a key role in many biologic and pathologic processes, such as embryogenesis, mitosis, and motility. Force changes in the adhesion and stiffness of cell surfaces have been measured for cell–cell and cell–ECM interaction with AFM[27,40–42]. Adhesion proteins distributed among the cellular membrane, especially as chondrocytes, mediate the capacity of the cell to make specific contact with the ECM.

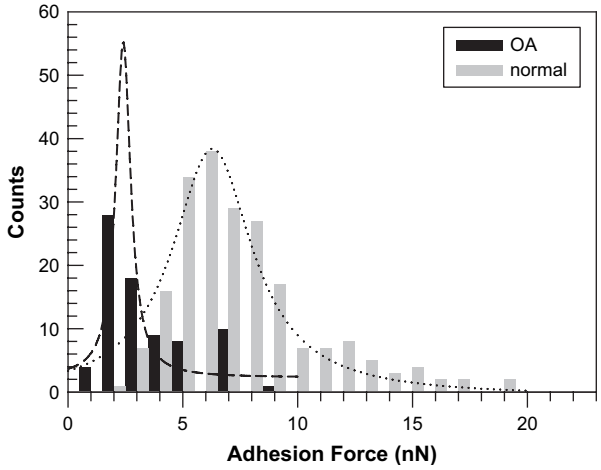

Fig. 5. Histograms and Gaussian distribution curves show differences in the adhesion forces of OA and normal chondrocytes; counts were 80 and 250, respectively. Measurements were based on a 10×10-μm scanned area.

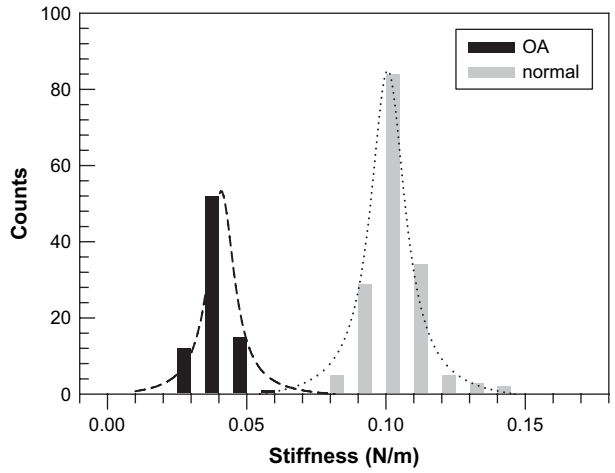

Fig. 6. Histograms and Gaussian distribution curves show stiffness measurements of OA and normal chondrocytes; counts were 80 and 250, respectively. Measurements were calculated from the slope of the approach curve.

In our research, OA chondrocytes had a low adhesion force of 2.97 ± 1.82 nN, whereas normal chondrocytes had a high adhesion force of 7.06 ± 3.35 nN. Adhesion forces of OA chondrocytes were relatively low and distributed over a narrow range compared with normal chondrocytes. Because the cellular adhesion force involves the collective behavior of individual proteins, the expression of membrane proteins of OA chondrocytes that interact with AFM probe is low. In addition, integrins are cell-surface transmembrane glycoproteins that function as adhesion receptors in ECM interactions and link the matrix proteins to the cytoskeleton. They play the functional role of adhesion to induce intracellular signaling mechanisms that regulate differentiation, cell polarity, proliferation, and apoptosis[14,43]. Integrins are a family of heterodimeric adhesion-related protein. Expression of $\alpha 1\beta 1$, $\alpha 2\beta 1$, $\alpha 5\beta 1$, $\alpha 6\beta 1$, $\alpha 10\beta 1$, $\alpha v\beta 3$ and $\alpha v\beta 5$ integrins in chondrocytes mediated the binding to type II collagen, fibronectin, vitronectin and laminin in the cartilage. The integrin $\beta 1$ was expressed abundant in the chondrocytes that might help to anchor the contracting actin cytoskeleton to the cell membrane. In addition, the integrin $\beta 1$ mediated chondrocyte–ECM interactions decrease in OA cartilage suggesting that perturbations of cell–matrix signaling occur during OA process[44]. In our results [Fig. 7(A) and (B)], the OA chondrocytes seemed to express few of integrin $\beta 1$ and normal chondrocytes (young modulus) have increased expression of integrin $\beta 1$. The expression of integrin $\beta 1$ fits in with measurement of AFM. Normal chondrocytes were more stable than old chondrocytes and highly adherent to the surface, which seemed to indicate a healthy cellular status.

Force–distance curves can provide information about another mechanical property, namely, stiffness, which is the mechanical parameter that describes the relation between an applied and nondestructive load and the resultant deformation of a chondrocyte. It can be determined at all scales of the internal structure of the cell, such as collagens, proteoglycans, glycoproteins, lipoglycans, and various macromolecules distributed around the cellular membrane. These macromolecules regulate number of important processes, including cellular proliferation, cellular differentiation, cellular migration, cell–cell interaction, cell–ECM interaction, and tissue–organ morphogenesis.

Stiffness measurements were three-fold higher in normal chondrocytes (0.0960 ± 0.009 N/m) than in old, OA chondrocytes (0.0347 ± 0.005 N/m), on average. When we

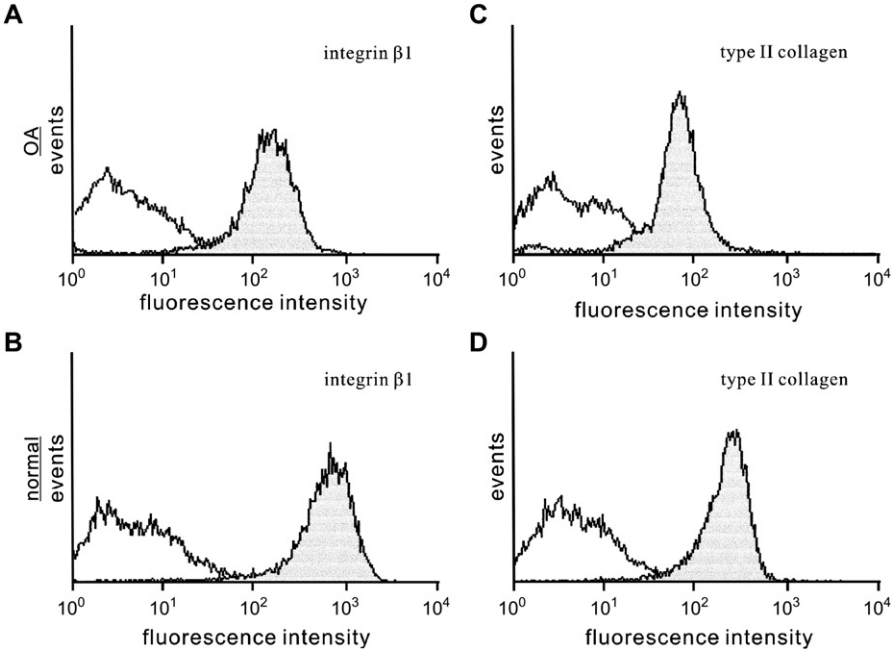

Fig. 7. Fluorescence-activated cell-sorting (FACS) analysis of integrin $\beta 1$ and type II collagen expression in the OA chondrocytes and in the normal chondrocytes. Donor: OA chondrocytes from 81-year-old patient, and normal chondrocytes from 24-year-old female. Histograms show the expression of integrin $\beta 1$ (A and B) and type II collagen (C and D) in OA and normal chondrocytes. White curves: negative controls, gray curves: mAb-FITC or mAb-PE labeled cells. Abscissa: cell fluorescence intensity. Ordinates: events (cells) observed by the flow cytometer.

compared stiffness histograms (Fig. 6), findings for normal chondrocytes revealed broadening of the distribution, with increasing stiffness and increasing complexity (mean roughness, 631.7 ± 171.7) of the sample surface. The lowered stiffness of OA chondrocytes (old modulus) was considered an effect of proteoglycan shortage due to a decreased rate of proteoglycan synthesis[23,45]. In addition, type II collagen forms the network of fibrils within which the proteoglycans are contained. Type II collagen of the chondrocytes plays the functional role as tensile strength in the cartilage[19,46]. In our data [Fig. 7(C) and (D)], the normal chondrocytes (young modulus) have expressed type II collagen higher than the OA chondrocytes (old modulus). These seem to fit within AFM observation. The variety of surface protein expression (integrin β1 and type II collagen) might make adhesion force and the stiffness difference between OA and normal chondrocytes.

In summary, we described a useful method for assessing the detailed structure of chondrocytes in old and young moduli by using an AFM. We obtained images of chondrocytes from single-cell measurements with AFM. The different structural parameters were all measured to distinguish OA and normal chondrocytes on a micrometer-to-nanometer scale. This technique can provide important information for engineering of cartilaginous tissue and for biologic research. Moreover, mechanical properties, adhesion forces, and stiffness were directly measured by using a mechanical probe at the same time. Correlations between nano-scale structure and mechanical properties were observed. We have shown how we can obtain morphologic data about biologic samples and compare mechanical changes in OA and normal chondrocytes related to disease of the articular cartilage.

Acknowledgments

This study was supported by the National Science Council (NSC 94-2314-B-002-093). The AFM was provided by Center for Optoelectronic Biomedicine, Institute of Applied Mechanics, National Taiwan University, Taipei, Taiwan. We would like to thank the staff of the Second Core Laboratory, Department of Medical Research, National Taiwan University Hospital for its technical support.

References

1. Dudhia J. Aggrecan, aging and assembly in articular cartilage. Cell Mol Life Sci 2005;62:2241–56.
2. Tyyni A, Karlsson J. Biological treatment of joint cartilage damage. Scand J Med Sci Sports 2000;10:249–65.
3. Stoltz JF, Netter P, Huselstein C, de Isla N, Wei Yang J, Muller S. Chondrocyte mecanobiology. Application in cartilage tissue engineering. Bull Acad Natl Med 2005;189:1803–14 (discussion 1814–1806).
4. Buckwalter JA, Mankin HJ. Articular cartilage: degeneration and osteoarthritis, repair, regeneration, and transplantation. Instr Course Lect 1998;47:487–504.
5. Buckwalter JA, Mankin HJ. Articular cartilage: tissue design and chondrocyte–matrix interactions. Instr Course Lect 1998;47:477–86.
6. Lohmander LS, Lark MW, Sandy JD. Mechanisms of degradation of argecanes in osteoarthritic cartilage. Rev Prat 1996;46:S11–4.
7. Lohmander LS, Neame PJ, Sandy JD. The structure of aggrecan fragments in human synovial fluid. Evidence that aggrecanase mediates cartilage degradation in inflammatory joint disease, joint injury, and osteoarthritis. Arthritis Rheum 1993;36:1214–22.
8. Mitani H, Takahashi I, Onodera K, Bae JW, Sato T, Takahashi N, *et al*. Comparison of age-dependent expression of aggrecan and ADAMTSs in mandibular condylar cartilage, tibial growth plate, and articular cartilage in rats. Histochem Cell Biol 2006.
9. Sandy JD, Flannery CR, Neame PJ, Lohmander LS. The structure of aggrecan fragments in human synovial fluid. Evidence for the involvement in osteoarthritis of a novel proteinase which cleaves the Glu 373–Ala 374 bond of the interglobular domain. J Clin Invest 1992;89:1512–6.
10. Buckwalter JA. Articular cartilage injuries. Clin Orthop Relat Res 2002; 21–37.
11. Forriol F, Shapiro F. Bone development: interaction of molecular components and biophysical forces. Clin Orthop Relat Res 2005; 14–33.
12. Kim HT, Lo MY, Pillarisetty R. Chondrocyte apoptosis following intraarticular fracture in humans. Osteoarthritis Cartilage 2002;10:747–9.
13. Loening AM, James IE, Levenston ME, Badger AM, Frank EH, Kurz B, *et al*. Injurious mechanical compression of bovine articular cartilage induces chondrocyte apoptosis. Arch Biochem Biophys 2000;381: 205–12.
14. Loeser RF. Integrins and cell signaling in chondrocytes. Biorheology 2002;39:119–24.
15. Hynes RO. Integrins: versatility, modulation, and signaling in cell adhesion. Cell 1992;69:11–25.
16. Kurtis MS, Schmidt TA, Bugbee WD, Loeser RF, Sah RL. Integrin-mediated adhesion of human articular chondrocytes to cartilage. Arthritis Rheum 2003;48:110–8.
17. Buckwalter JA, Mankin HJ, Grodzinsky AJ. Articular cartilage and osteoarthritis. Instr Course Lect 2005;54:465–80.
18. Eyre DR, Wu JJ, Fernandes RJ, Pietka TA, Weis MA. Recent developments in cartilage research: matrix biology of the collagen II/IX/XI heterofibril network. Biochem Soc Trans 2002;30:893–9.
19. Poole AR, Kojima T, Yasuda T, Mwale F, Kobayashi M, Laverty S. Composition and structure of articular cartilage: a template for tissue repair. Clin Orthop Relat Res 2001;S26–33.
20. Schmal H, Mehlhorn AT, Fehrenbach M, Muller CA, Finkenzeller G, Sudkamp NP. Regulative mechanisms of chondrocyte adhesion. Tissue Eng 2006;12:741–50.
21. van der Kraan PM, Buma P, van Kuppevelt T, van den Berg WB. Interaction of chondrocytes, extracellular matrix and growth factors: relevance for articular cartilage tissue engineering. Osteoarthritis Cartilage 2002;10:631–7.
22. Solchaga LA, Goldberg VM, Caplan AI. Cartilage regeneration using principles of tissue engineering. Clin Orthop Relat Res 2001; S161–70.
23. Martin JA, Buckwalter JA. Aging, articular cartilage chondrocyte senescence and osteoarthritis. Biogerontology 2002;3:257–64.
24. Binnig G, Quate CF, Gerber C. Atomic force microscope. Phys Rev Lett 1986;56:930–3.
25. Darling EM, Zauscher S, Guilak F. Viscoelastic properties of zonal articular chondrocytes measured by atomic force microscopy. Osteoarthritis Cartilage 2006;14(6):571–9.
26. Ganguli M, Babu JV, Maiti S. Complex formation between cationically modified gold nanoparticles and DNA: an atomic force microscopic study. Langmuir 2004;20:5165–70.
27. Lesniewska E, Milhiet PE, Giocondi MC, Le Grimellec C. Atomic force microscope imaging of cells and membranes. Methods Cell Biol 2002;68:51–65.
28. Scott CC, Luttge A, Athanasiou KA. Development and validation of vertical scanning interferometry as a novel method for acquiring chondrocyte geometry. J Biomed Mater Res A 2005;72:83–90.
29. Wu Y, Cai J, Cheng L, Xu Y, Lin Z, Wang C, *et al*. Atomic force microscope tracking observation of Chinese hamster ovary cell mitosis. Micron 2006;37:139–45.
30. Stolz M, Raiteri R, Daniels AU, VanLandingham MR, Baschong W, Aebi U. Dynamic elastic modulus of porcine articular cartilage determined at two different levels of tissue organization by indentation-type atomic force microscopy. Biophys J 2004;86:3269–83.
31. Lee HS, Huang GT, Chiang H, Chiou LL, Chen MH, Hsieh CH, *et al*. Multipotential mesenchymal stem cells from femoral bone marrow near the site of osteonecrosis. Stem Cells 2003;21:190–9.
32. Kempson GE. Age-related changes in the tensile properties of human articular cartilage: a comparative study between the femoral head of the hip joint and the talus of the ankle joint. Biochim Biophys Acta 1991;1075:223–30.
33. Buckwalter JA, Martin J, Mankin HJ. Synovial joint degeneration and the syndrome of osteoarthritis. Instr Course Lect 2000;49:481–9.
34. Koepp H, Eger W, Muehleman C, Valdellon A, Buckwalter JA, Kuettner KE, *et al*. Prevalence of articular cartilage degeneration in the ankle and knee joints of human organ donors. J Orthop Sci 1999;4:407–12.
35. Verzijl N, DeGroot J, Ben ZC, Brau-Benjamin O, Maroudas A, Bank RA, *et al*. Crosslinking by advanced glycation end products increases the stiffness of the collagen network in human articular cartilage: a possible mechanism through which age is a risk factor for osteoarthritis. Arthritis Rheum 2002;46:114–23.
36. Bolton MC, Dudhia J, Bayliss MT. Age-related changes in the synthesis of link protein and aggrecan in human articular cartilage: implications for aggregate stability. Biochem J 1999;337(Pt 1):77–82.

37. Dozin B, Malpeli M, Camardella L, Cancedda R, Pietrangelo A. Response of young, aged and osteoarthritic human articular chondrocytes to inflammatory cytokines: molecular and cellular aspects. Matrix Biol 2002;21:449–59.
38. Messai H, Duchossoy Y, Khatib AM, Panasyuk A, Mitrovic DR. Articular chondrocytes from aging rats respond poorly to insulin-like growth factor-1: an altered signaling pathway. Mech Ageing Dev 2000;115: 21–37.
39. Rosen F, McCabe G, Quach J, Solan J, Terkeltaub R, Seegmiller JE, *et al*. Differential effects of aging on human chondrocyte responses to transforming growth factor beta: increased pyrophosphate production and decreased cell proliferation. Arthritis Rheum 1997;40:1275–81.
40. Matzke R, Jacobson K, Radmacher M. Direct, high-resolution measurement of furrow stiffening during division of adherent cells. Nat Cell Biol 2001;3:607–10.
41. Radmacher M. Measuring the elastic properties of living cells by the atomic force microscope. Methods Cell Biol 2002;68:67–90.
42. Schneider SW, Matzke R, Radmacher M, Oberleithner H. Shape and volume of living aldosterone-sensitive cells imaged with the atomic force microscope. Methods Mol Biol 2004;242:255–79.
43. Brakebusch C, Fassler R. Beta 1 integrin function *in vivo*: adhesion, migration and more. Cancer Metastasis Rev 2005;24:403–11.
44. Lapadula G, Iannone F, Zuccaro C, Grattagliano V, Covelli M, Patella V, *et al*. Chondrocyte phenotyping in human osteoarthritis. Clin Rheumatol 1998;17:99–104.
45. DeGroot J, Verzijl N, Bank RA, Lafeber FP, Bijlsma JW, TeKoppele JM. Age-related decrease in proteoglycan synthesis of human articular chondrocytes: the role of nonenzymatic glycation. Arthritis Rheum 1999;42:1003–9.
46. Mayne R. Cartilage collagens. What is their function, and are they involved in articular disease? Arthritis Rheum 1989;32:241–6.
47. Pfeuty A, Gueride M. Peroxide accumulation without major mitochondrial alteration in replicative senescence. FEBS Lett 2000 Feb 18; 468(1):43–7.